Experimental and Theoretical Investigation of the First-Order Hyperpolarizability of Octupolar Merocyanine Dyes

ARTICLE *in* CHEMPHYSCHEM · AUGUST 2014

Impact Factor: 3.42 · DOI: 10.1002/cphc.201402083 · Source: PubMed

6 AUTHORS, INCLUDING:

Frédéric Castet
Université of Bordeaux
90 PUBLICATIONS **1,693** CITATIONS
SEE PROFILE

Daniel Gryko
Polish Academy of Sciences
215 PUBLICATIONS **3,494** CITATIONS
SEE PROFILE

Vincent Rodriguez
University of Bordeaux
172 PUBLICATIONS **1,921** CITATIONS
SEE PROFILE

ChemPubSoc Europe

DOI: 10.1002/cphc.201402083

Experimental and Theoretical Investigation of the First-Order Hyperpolarizability of Octupolar Merocyanine Dyes

Frédéric Castet,[a] Mireille Blanchard-Desce,[a] Frédéric Adamietz,[a] Yevgen M. Poronik,[b] Daniel T. Gryko,[b] and Vincent Rodriguez*[a]

Hyper-Rayleigh scattering experiments and quantum chemical calculations are combined to investigate the second-order nonlinear optical responses of a series of three-arm merocyanine derivatives. They exhibit an octupolar hyperpolarizability response with lower amplitude than crystal violet due to a lower extent of the photoinduced charge transfer and reduced bond length alternation. Strong effects on the second-order optical response measured close to the two-photon absorption level are clearly evidenced; for example, the effective measured polarization ratio deviates below the ideal octupolar value of 3/2 even at very low excitation power. These effects are attributed to two-photon absorption resonance, which we believe modifies dynamically the population of the ground state versus that of the excited state.

1. Introduction

Molecular nonlinear optics (NLO) has been a subject of continuous interest in the past few decades in connection with various applications in different fields ranging from materials science (optical telecommunications, 3D data storage, fast information and signal processing, microfabrication, etc.)[1] to biology (including in vivo bioimaging[2] and therapy[3]). This has motivated numerous experimental and theoretical studies aiming at the design of organic compounds with large NLO responses and optimized properties. In particular, the design of molecular compounds having enhanced second-order polarizability (or first-order hyperpolarizability) β has been very active, mainly driven by their use as components for the fabrication of electro-optic devices[4] and more recently as nonlinear probes for cellular imaging.[5]

Among various compounds, octupolar chromophores[6] have attracted particular attention for both their second-order[6] and third-order[2h] optical responses. Interestingly, whereas there have been countless efforts in the optimization of the NLO dipolar derivatives for electro-optics (EO), octupolar derivatives have been much less investigated in this regard. Yet, compared to their dipolar counterparts, they possess several characteristics that are quite favorable for EO: increased transparency, absence of dipole moment, and insensitivity to polarization.[6] Among octupolar derivatives, two-dimensional derivatives with ternary symmetry have proven to be of major interest, leading to potentially very high β values (Figure 1). These derivatives, with crystal violet (**CV**) as the prototypical compound, are generally built from either an electron-withdrawing core (such as tricyano or trinitrobenzene, triazines, isocyanurates, boroxines, truxenone etc.)[6c,7] or an electron-donating core (trimethoxybenzene, triphenylbenzene, triphenylamine etc.).[6c]

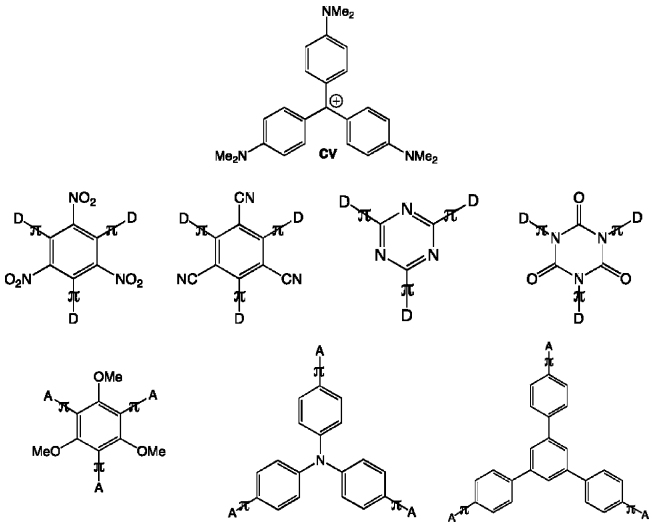

Figure 1. Structure of the prototypical octupole crystal violet (**CV**, top) and examples[6c] of ternary octupoles built from an electron-withdrawing core (middle) or electron-donating core (bottom).

A four-state model has been used earlier to describe the hyperpolarizability β of simple ternary systems derived from **CV**, which indicates that their hyperpolarizability can be increased significantly by increasing the intramolecular charge transfer (CT) in the ground state (i.e. the contribution of the CT forms).[8] Strikingly, most common two-dimensional octupolar

[a] Dr. F. Castet, Dr. M. Blanchard-Desce, F. Adamietz, Prof. Dr. V. Rodriguez
Institut des Sciences Moléculaires, CNRS UMR5255
Université de Bordeaux
351 Cours de la Libération, 33405 Talence (France)
E-mail: vincent.rodriguez@u-bordeaux.fr

[b] Y. M. Poronik, Prof. Dr. D. T. Gryko
Institute of Organic Chemistry of the Polish Academy of Sciences
Kasprzaka 44/52, 01-224 Warsaw (Poland)

Supporting Information for this article is available on the WWW under http://dx.doi.org/10.1002/cphc.201402083.

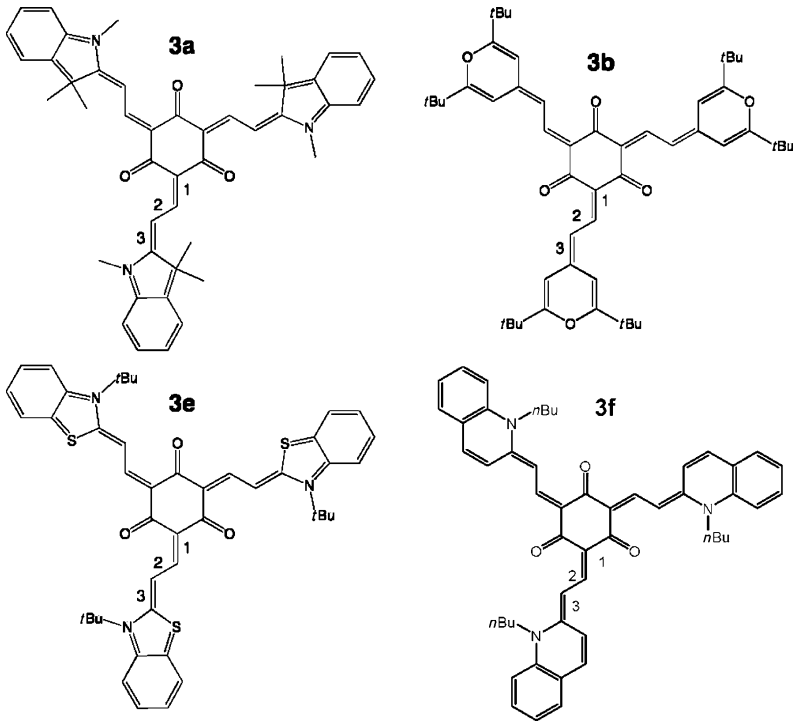

Figure 2. Molecular structures of merocyanine octupoles.[9]

derivatives possess an aromatic core and subsequent low intramolecular CT in the ground state. Hence pronounced variation of bond length alternation (BLA) cannot be achieved by simple variation of substituent strength. Recently, we have studied a new class of octupolar merocyanines that were shown to exhibit high two-photon absorption responses in the near-IR range (with varying amplitude depending on ground-state structure)[9] and with a structure that could be tuned closer to the cyanine limit (Figure 2). Herein, we investigate both experimentally and theoretically the variation of BLA and second-order polarizability in this series, and show that the amount of intramolecular CT significantly affects the second-order responses.

2. Results and Discussion

2.1. Molecular Structures and Linear Absorption Properties

The optimized structures of the four merocyanine compounds are reported in Figure S1 (see the Supporting Information), whereas the characteristics of the two degenerate excited states S_1 and S_2 accessible by one-photon absorption are provided in Table 1, along with results obtained for the **CV** reference molecule. We stress that all merocyanine compounds show a planar structure (in contrast with **CV**, in which the phenyl groups are twisted by an angle of 33°). Although the $S_0 \rightarrow S_1$ transition energies calculated at the LC-BLYP/6-311G(d) level are systematically blue-shifted by approximately 1 eV compared with the experimental values, the relative ΔE values follow the same hierarchy (**3 f** < **3 b** < **3 e** < **CV** < **3 a**). The oscillator strengths of the four merocyanines are significantly larger than those calculated for **CV**, with **3 b** and **3 f** exhibiting slightly larger transition probabilities than the **3 a** and **3 e** derivatives.

As an indication of the extent of electron conjugation along the branches of the molecules, Table 1 also reports the bond length alternation (BLA $= d_1 + d_3 - 2d_2$, see Figure 2 for bond labels) along the ethylenic bridge connecting the central aromatic core to the external substituents. The BLA values of the merocyanine compounds follow the same hierarchy (**3 f** < **3 b** ≈ **3 e** < **3 a**) as the transition energies. Moreover, to gain insight into the CT process occurring upon photoexcitation of the dyes, the amount of charge transferred (q^{CT}) and the CT distance (d^{CT}, that is, the spatial extent of the charge delocalization) were evaluated from the difference $\Delta\rho$ between the ground- and excited-state electron densities by using the procedure described in ref. [10]. In this procedure, $\Delta\rho$ is split into two contributions, ρ^+ and ρ^-, which correspond respectively to positive and negative areas of the density variation. The amount of charge transferred, q^{CT}, is defined as the integral over space of the ρ^+ (or ρ^-) function, whereas d^{CT} is the distance separating the barycenters of the ρ^+ and ρ^- functions. The light-induced dipole moment variation, the norm of which is defined as $\mu^{CT} = q^{CT} \times d^{CT}$, is also reported. Note that by symmetry the $S_0 \rightarrow S_2$ transition leads to a dipole variation μ^{CT} of same amplitude as $S_0 \rightarrow S_1$ with opposite direction. Similar values of q^{CT} and d^{CT} are obtained for **3 b** and **3 e**, whereas **3 a**

Table 1. Bond length alternation (BLA) [Å] along the ethylenic bridge, transition energies ΔE [eV], transition wavelengths λ [nm], oscillator strengths f, charge transferred q^{CT} [|e|], CT distance d^{CT} [Å], and dipole moment variation μ^{CT} [D] calculated for the $S_0 \rightarrow S_1$ transition at the LC-BLYP/6-311G(d) level. Experimental absorption maxima results, λ_{max} [nm] and ΔE_{max} [eV], and molar extinction coefficients ε [$M^{-1}cm^{-1}$] are reported in the last three lines.

	3 a	3 b	3 e	3 f	CV
λ	420	460	445	477	438
ΔE	2.952	2.695	2.784	2.599	2.833
f	1.950	2.162	1.955	2.305	1.197
BLA	0.075	0.062	0.063	0.036	–
q^{CT}	0.615	0.580	0.601	0.575	0.697
d^{CT}	0.863	0.859	0.842	0.436	2.077
μ^{CT}	2.719	2.427	2.450	1.254	7.019
λ_{max}	574	636	603	659	588
ΔE_{max}	2.160	1.949	2.056	1.881	2.108
ε	172 000	131 000	215 000	213 000	107 000

displays slightly larger q^{CT} and d^{CT} values, which give rise to a larger dipole moment variation. The amount of charge transferred for **3 f** is similar to that calculated for the three other merocyanines; however, the CT distance is twice as short, which reduces the μ^{CT} value by a factor of 2. On the other hand, the photoinduced CT is highly efficient in **CV**, thus leading to a dipole variation much larger than that calculated for the four merocyanines.

2.2. Nonlinear Optical Properties

Typical 3D representations of the hyper-Rayleigh scattering (HRS) responses of merocyanine dye **3 f** and **CV** as a function of the incident power and concentration of dye, as well as polarization curves of the solvated dyes, are reported in Figure 3. The corresponding details for the other compounds are supplied in the Supporting Information.

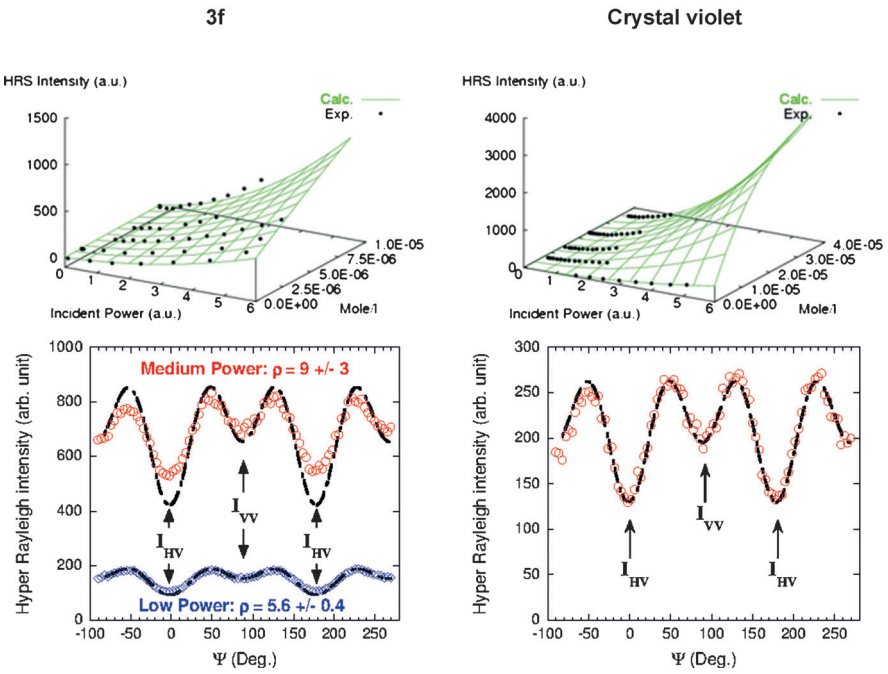

Figure 3. HRS responses of **3 f** (left) and **CV** (right): 3D representation as a function of the incident power and concentration (top) and extracted polarization curve of the solvated dyes (bottom). Points, circles, and squares are experimental data and solid lines are the best-fitted curves according to Equation (1) (top) and Equation (2) (bottom) (see the Experimental and Theoretical Section). The polarization curves of **3 f** differ at low power (bottom curve) and medium power (top curve), at which a deviation from the expected law is observed.

As expected, the HRS polarization curves of **CV** and **3 f** are typical of octupolar dyes, with high anisotropy factors ($\rho > 5$). However, Figure 3 evidences a strong effect of the incident power on the shape of the polarization curve of **3 f**, which gives rise to different (effective) anisotropy factors ρ at low and medium power. In addition, the experimental curve of **3 f** deviates significantly from the expected law at medium power. Similar deviations with laser power are observed for the three other merocyanine derivatives (Figure S2). As all these dyes display high two-photon absorption (TPA) cross sections,[9] these discrepancies are attributed to third-order NLO contributions. Figure S3 a reports the two-photon excited fluorescence (TPEF) spectra of **3 f**, which differ slightly at low and medium power.

We suspect that during laser irradiation, above a critical power level, the octupolar merocyanines undergo a transitory regime in which one (or few) exited state(s) is (are) dynamically populated, to the detriment of the electronic ground-state population. In addition, we have observed on the charge-coupled device (CCD) image that the corresponding TPEF spot splits into two parts along the spatial direction at medium power, that is, the inner part of the spot (where the excitation power is maximal) decreases significantly (Figure S3 b). However, despite that splitting, the spatial position of the center of the spot does not change with power, which indicates that no optical Kerr effect occurs.[1] To summarize, these observations point out that light irradiation very close to the TPA resonance of the dyes involves the imaginary part of the third-order NLO contribution, which strongly perturbs the second-order measurements. Another illustration of this phenomenon is given Figure S4, in which the as-measured depolarization ratio (DR) of **3 f** may deviate from the expected octupolar value of 1.5 (by decreasing up to $\approx$1.2) even at relatively low power. Detailed investigations of the perturbation due to third-order NLO effects on the HRS signal are, however, out of the scope of the present paper and will be the subject of further studies. To minimize these effects, experimental data were obtained using an incident laser power as low as possible but high enough to enable reliable signal-to-noise detection. As a consequence, slight deviations from the expected polarization curves can be detected (see Figure S2), which lowers the experimental accuracy of the extracted HRS hyperpolarizabilities. These latter are reported in Table 2 (according to the T Convention)[11] along with the spherical β_J components and the associated depolarization and ρ ratios.

The measured β_{HRS} values of the merocyanine compounds evolve in the order **3 a** < **3 e** < **3 b** < **3 f**, that is, the reverse order of the transition energies. Hence reduction of BLA leads to increased first hyperpolarizability. Such a trend is consistent with the trends predicted on the basis of valence bond states

[1] *The optical Kerr effect involves the real part of the third-order NLO contribution, which modifies (linearly) the total effective index of refraction of the solution at the focal plane with respect to the incident power.*

Table 2. β_{HRS} and β_J values (in 10^3 atomic units,[a] using Convention T) and ratios deduced from HRS measurements at 1064 nm in $HCCl_3$. Relative β_{HRS} values with respect to **CV** are reported in parentheses.

	3a	3b	3e	3f	CV
β_{HRS}	22 ± 4 (0.44)	33.2 ± 1.5 (0.66)	25.8 ± 1.5 (0.52)	36.8 ± 1.5 (0.74)	50 ± 2 (1.00)
ρ	2.7 ± 0.1	5.7 ± 0.4	5.1 ± 0.7	5.6 ± 0.4	≫ 10
$\beta_{J=1}$	23.3	18.3	15.7	20.6	0.9
$\beta_{J=3}$	62	104	80.1	115.1	162.2
DR[b]	2.07	1.63	1.66	1.64	1.50

[a] 1 atomic unit of $\beta = 3.62 \times 10^{-42}$ $m^4 V^{-1} = 8.641 \times 10^{-33}$ esu. [b] Calculated using Equation (3) defined in the Experimental and Theoretical Section.

Table 3. Dynamic ($\lambda = 1064$ nm) HRS hyperpolarizabilities (in atomic units, using Convention T) and depolarization ratios (DRs) calculated at the TD-HF and TD-DFT levels with the 6-311 + G(d) basis set. Solvent effects (chloroform) are included using the IEF-PCM model.

TD-HF	3a	3b	3e	3f	CV
β_{HRS}	5638 (0.38)	9582 (0.65)	6349 (0.43)	16250 (1.09)	14849 (1.00)
ρ	73	910	57	84	146
$\beta_{J=1}$	250	34.13	364	630	330
$\beta_{J=3}$	18265	31049	20565	52647	48117
DR	1.50	1.50	1.50	1.50	1.50
TD-DFT	**3a**	**3b**	**3e**	**3f**	**CV**
β_{HRS}	11038 (0.32)	17637 (0.51)	14265 (0.42)	20000 (0.58)	34259 (1.00)
ρ	40	580	42	136	132
$\beta_{J=1}$	901	99	1099	477	841
$\beta_{J=3}$	35740	57152	46195	64804	111021
DR	1.50	1.50	1.50	1.50	1.50

modeling for triphenylmethane derivatives.[8] The highest first hyperpolarizability within the series, obtained for **3f**, corresponds to 75% of the response of the **CV** reference, although this latter exhibits a smaller maximum absorption wavelength than **3f**. As discussed above, the larger β_{HRS} response of **CV** is related to the larger extent of the photoinduced CT upon the $S_0 \rightarrow S_1$ transition, which gives rise to a dipole moment variation about five times larger than that of **3f**. Quite equivalent to **CV**, polarization ratios of about 1.6, typical of octupolar chromophores, are measured for **3b**, **3e**, and **3f**. The DR value measured for **3a** deviates more substantially from the ideal octupolar response to approximately 2.1, which is, as discussed above, attributed to third-order processes that contaminate the HRS signal. This deviation is indeed more pronounced in the case of **3a**, for which a strong effect of the incident power is also detected in the 3D representation of the HRS intensity versus the incident power and concentration (Figure S2). Note that **3a** exhibits linear and two-photon absorptions with maxima close to the HRS response at 532 nm.[9]

The dynamic β_{HRS} and β_J values calculated at the time-dependent Hartree–Fock (TD-HF) and time-dependent density functional theory (TD-DFT) levels in chloroform, as well as the associated ratios, are gathered in Table 3. To disentangle the contributions due to frequency dispersion and solvent effects from the intrinsic (static gas phase) NLO responses of the molecules, both static and dynamic results, computed in the gas phase or in solvent, are provided in the Supporting Information. The enhancement due to frequency resonance, evaluated at the TD-HF level as the ratio between the dynamic and static gas-phase β_{HRS} values, lies in the range 1.4–1.9 for the merocyanine derivatives. Because TD-DFT calculations provide lower transition energies than TD-HF, frequency dispersion factors obtained at the TD-DFT level are larger than the TD-HF ones, and range between 2.7 (**3a**) and 6.3 (**3b**). Accounting for solvent effects also leads to an enhancement of the static β_{HRS} values by roughly a factor of 2, which is less sensitive to the nature of the chromophore. This solvent-induced enhancement is substantially reduced on consideration of the dynamic β_{HRS} values, since the dynamic dielectric constant of chloroform is smaller than the static one.

As reported in previous studies,[12] both the TD-HF and TD-DFT/LC-BLYP methods strongly underestimate the hyperpolarizability values of the investigated compounds. However, rather than considering the absolute values, the predictive power of these methods can be assessed by considering the relative β_{HRS} values. In contrast to experimental results, dynamic TD-HF calculations including solvent effects predict a β_{HRS} value for **3f** slightly larger than that of **CV**, yet providing the correct hierarchy in the HRS responses of the four merocyanines. Accounting for electron correlation effects at the TD-DFT/LC-BLYP level increases the β_{HRS} values of the merocyanine compounds by a factor ranging from 1.2 (**3f**) to 2.3 (**CV**), which leads to a good agreement with the experimental results regarding the relative β_{HRS} values. The calculated polarization ratios of all compounds are equal to 1.5, which differs slightly from experimental values, these latter being probably biased for the reasons evoked above.

3. Conclusions

We have investigated the HRS response of merocyanine dyes. As expected, these three-arm chromophores exhibit octupolar second-order responses, which are, however, lower than that measured for the octupolar prototype crystal violet. Interestingly, we observed that the HRS hyperpolarizability values increase continuously with decreasing BLA, which is a markedly different behavior from that of dipolar derivatives getting closer to the cyanine limit. Quantum chemical calculations performed at the TD-DFT level using the long-range-corrected LC-BLYP exchange-correlation functional reproduced well the relative values of the HRS hyperpolarizabilities, and allowed the lower first-order hyperpolarizability of the merocyanine derivatives to be attributed to a lower extent of photoinduced CT upon the $S_0 \rightarrow S_1$ transition. In addition, we have evidenced substantial deviations from the expected behavior of second-order optical responses, notably in the polarization curves on increasing the incident power, but existing even at very low power. These effects are attributed to third-order NLO contributions, more precisely to two-photon absorption resonance

that in our opinion dynamically modifies the relative electron population of the ground versus excited states.

Experimental and Theoretical Section

Hyper-Rayleigh Scattering

HRS measurements were performed with diluted solutions (with concentrations ranging from 5×10^{-5} to 10^{-6} M) in chloroform, which has also been used as an internal reference.[13] Measurements were also performed on crystal violet (**CV**) diluted in chloroform, since it is a well-known prototype of the NLO octupolar molecule.[6a,b,14] The experimental setup is configured in a classical 90° scattering geometry for HRS detection (Figure 4).

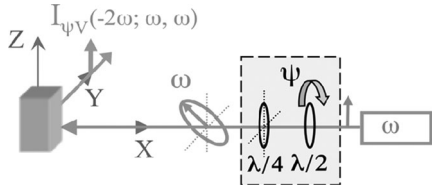

Figure 4. Sketch of the experimental HRS setup.

The incident radiation at 1064 nm was obtained from a Nd:YVO_4 laser that produced trains of about 65 ps, $\leq$50 μJ pulses at a repetition rate of 2 kHz (PL2200 Laser, EKSPLA). The elliptical polarization of the incident light denoted by the polarization angle Ψ was obtained by using a combination of a rotating half-wave plate ($\lambda/2$) and a fixed quarter-wave plate ($\lambda/4$). All elliptical states of polarization of the incident light could be obtained as well as linear polarization H ($\Psi=0°$) and V ($\Psi=90°$) and left/right circular polarization ($\Psi=\pm45°$). The polarized incident laser beam was focused into the sample cell with a 5X Mitutoyo Plan APO NIR objective (infinity-corrected with NA = 0.14) and positioned to pass at a distance of 1–2 mm from the inside of the cell wall facing the collecting lens. The incident laser beam waist had a diameter of approximately 10 μm with a Rayleigh range of about 200 μm. The scattered light at the double frequency (532 nm) was collected at 90° with f/1.7 optics and focused into a modified Horiba spectrograph, with vertical (V) polarization selection.[15] The entrance slits of the spectrograph were closed to fit the full beam waist image. The spectrally dispersed light (using an 1800 grooves per mm grating), detected by a nitrogen-cooled CCD camera (2048×512 pixels) in a continuous acquisition mode, was collected around the 532 nm harmonic light scattering and covered a spectral range of about 1800 cm^{-1} with a spectral slit width of about 15 cm^{-1} (spectral binning mode). The spatial resolution was estimated using the CCD image mode and, in any case, the HRS signal was confined to dimensions less than the Rayleigh range (<200 μm) so that no correction for the effect of a finite collection angle was required. This setup has also been used successfully for hyper-Raman and Raman studies of several liquids, glasses, and crystals.[16–18] Because of the strong two-photon absorption (TPA)[9] of these dyes, the range of incident power was limited to very low excitation values (less than 10 μJ $pulse^{-1}$) to minimize all third-order NLO contributions to the whole collected signal. As a consequence, typical acquisition times to acquire good signal-to-noise spectra ranged between 20 and 30 s. The hyper-Rayleigh intensity was obtained by integrating the signal from -200 to $+200$ cm^{-1} after eliminating the background, which was extrapolated by a linear law obtained by excluding this spectral range.

For the study of isotropic media and particularly liquids, it is convenient to evoke the irreducible spherical representations of the hyperpolarizability β tensor and to use the mixed spherical–Cartesian formalism to discuss HRS measurements in terms of multipolar components.[19] Indeed, the use of spherical invariants allows the β tensor (symmetric rank-3 tensor) to be decomposed as the sum of dipolar ($\beta_{J=1}$) and octupolar ($\beta_{J=3}$) tensorial components, as illustrated recently in HRS investigations of molecular and ionic liquids,[13,20] or silica glass.[17] In that multipolar description, the total harmonic scattered light for a binary solution (solvent/chromophore) in the diluted regime is given by [Eq. (1)]

$$I_{\psi V}^{2\omega} = Gf_L^2\left[\left\{C_S\left[|\beta_{J=1}|^2 C_{\psi V}\right]_S\right\} + C_X\left[|\beta_{J=1}|^2 C_{\psi V}\right]_X\right]\cdot 10^{-(\alpha_{2\omega}+\sigma_\omega I^\omega)C_X}\cdot [I^\omega]^2 \quad (1)$$

in which the subscripts S and X respectively stand for the solvent and the chromophore; G is a constant containing geometrical, optical, and electrical factors of the experimental setup; C is the concentration (molarity) of the solvent or solute; $\alpha_{2\omega}$ accounts for one-photon absorption of the total harmonic response from the chromophore; and $\sigma_\omega I^\omega$ accounts for two-photon absorption of the chromophore at the fundamental frequency when necessary. $f_L = \left((n_\omega^2+2)/3\right)^2\left((n_{2\omega}^2+2)/3\right)$ is a local field correction approximated using the high-frequency Lorentz–Lorenz spherical cavity expression, which includes the refractive index of the solvent at the optical frequencies ω and 2ω. $C_{\psi V}$ is the orientational average of the molecular spherical components of the hyperpolarizability of the solute or solvent given by [Eq. (2)]

$$C_{\psi V}(i) = \left\{\begin{array}{c}\left(\frac{9}{45}+\frac{6}{105}\rho^2(i)\right)+\left(-\frac{20}{45}+\frac{10}{105}\rho^2(i)\right)\cos^2(\psi)\\ +\left(\frac{12}{45}-\frac{12}{105}\rho^2(i)\right)\cos^4(\psi)\end{array}\right\} \quad (2)$$

The nonlinear anisotropy $\rho = |\beta_{J=3}|/|\beta_{J=1}|$ compares the relative contributions of the octupolar and dipolar components of the hyperpolarizability tensor. The commonly used depolarization ratio (DR), defined as [Eq. (3)]

$$DR = I_{VV}/I_{HV} = 9[1+(2\rho^2)/7]/[1+(12\rho^2/7)] \quad (3)$$

is expected to be between 3/2 in the case of pure octupolar response and 9 for a pure dipolar response.

Thus, the measured HRS responses of the investigated dyes were analyzed using the internal method (the solvent response is the reference value) in a two-step procedure:

1) First, the macroscopic response of solute X, $|\beta_{J=1}|^2$, has been obtained by determining the coefficient of the quadratic dependence of the polarized HRS response on varying the incident intensity I^ω for different concentrations C_X [see Eq. (1)], for which $C_{VV} = (1/5+2\rho^2/35)$.
2) Second, polarization scans of the scattered light $I_{\psi V}^{2\omega}$ at constant incident power I^ω have been carried out for both the solvent and chromophore to determine the nonlinear anisotropy ρ(X) of the chromophore from a fitting procedure involving Equation (2). To obtain the solvated chromophore polarization

curve, we first applied corrections (if necessary) to account for one-photon absorption losses and/or modification of the irradiated volume due to TPA[2] at the harmonic response for the binary solution, before subtracting the solvent contribution to the total corrected HRS intensity.

From the knowledge of the relative dipolar/octupolar contributions to the hyperpolarizability tensor given by ρ, the orientational average of the chromophore C_{VV} was finally determined to obtain the dipolar tensorial component $|\beta_{J=1}|$, the octupolar one $|\beta_{J=3}| = \rho|\beta_{J=1}|$, and the total HRS intensity (obtained without polarization analysis of the scattered beam) $\beta_{HRS} = |\beta_{J=1}|\sqrt{2(1/3+\rho^2/7)/3}$.

Quantum Chemical Methods

Molecular geometries were optimized in vacuo at the density functional theory (DFT) level of approximation using the B3LYP hybrid exchange-correlation (XC) functional in combination with the 6-311G(d) basis set. The dynamic nonlinear optical responses were calculated using the time-dependent Hartree–Fock (TD-HF) method[21] with an incident wavelength of 1064 nm and the 6-311+G(d) basis set, since split-valence triple-zeta basis sets including one set of diffuse and polarization functions were shown to be sufficient to describe the dominant β-tensor components of the first hyperpolarizability tensor.[12,22] In addition, frequency-dependent hyperpolarizabilities were also calculated using the long-range-corrected LC-BLYP XC functional with a range separation parameter of 0.47. This functional has been shown to correct the shortsightedness drawbacks of conventional DFT schemes[23] for computing the NLO properties of conjugated molecules, while it allows handling of extended systems. In particular, the TD-DFT/LC-BLYP method has been proven suitable to describe the variations of β values induced by chemical modifications in extended π-conjugated systems.[12] TD-DFT calculations of β were performed using the (99, 590) integration grid, which involves 99 radial shells around each atom and 590 angular points in each shell. Note that our theoretical predictions concentrate uniquely on the electronic contribution of the first hyperpolarizability, because for the second harmonic generation process the pure vibrational response is negligible whereas the zero-point vibrational averaging is small.[24] Linear optical properties were calculated at the LC-BLYP/6-311G(d) level. Solvent effects on both linear and nonlinear optical responses were taken into account by using the integral equation formalism version of the polarizable continuum model (IEF-PCM). This model approximates the solvent as a structureless polarizable continuum characterized by its macroscopic dielectric permittivity ε, which depends on the frequency of the applied electric field. For chloroform, $\varepsilon_0 = 4.711$ in the static field limit, and $\varepsilon_\infty = 2.091$ at infinite frequency. All calculations were performed using the Gaussian 09 program.[25]

Acknowledgements

V.R. thanks the CNRS (Chemistry Department) and Région Aquitaine for providing financial support for equipment. Calculations were carried out on mainframe computers of the "Mésocentre de Calcul Intensif Aquitain" (MCIA) of Bordeaux University, financed by the Conseil Régional d'Aquitaine and the French Ministry of Research and Technology. M.B.-D. gratefully acknowledges the Conseil Régional d'Aquitaine for generous funding (Chaire d'Accueil grant). D.T.G. and Y.M.P. thank the Foundation for Polish Science (TEAM-2009-4/3).

Keywords: dyes/pigments · hyperpolarizability · merocyanines · nonlinear optics · quantum chemistry

[2] *The TPA perturbs strongly the distribution of intensity in the focused volume as reported in the Supporting Information (Figure S3). The intensity contribution of the solvent in the polarization curve of the binary solution is thus corrected from this chromophore third-order NLO effect before extracting the solvated chromophore polarization curve.*

[1] a) D. A. Parthenopoulos, P. M. Renzepis, *Science* **1989**, *245*, 843–845; b) C. C. Corredor, Z.-L. Huang, K. D. Belfield, A. R. Morales, M. V. Bondar, *Chem. Mater.* **2007**, *19*, 5165–5173.

[2] a) W. Denk, J. H. Strickler, W. W. Webb, *Science* **1990**, *248*, 73–76; b) C. Xu, W. Zipfel, J. B. Shear, R. M. Williams, W. W. Webb, *Proc. Natl. Acad. Sci. USA* **1996**, *93*, 10763–10768; c) D. R. Larson, W. R. Zipfel, R. M. Williams, S. W. Clark, M. P. Bruchez, F. W. Wise, W. W. Webb, *Science* **2003**, *300*, 1434–1436; d) R. K. Tathavarty, M. Parent, M. H. V. Werts, S. Gmouh, A.-M. Caminade, L. Moreaux, S. Charpak, J.-P. Majoral, M. Blanchard-Desce, *Angew. Chem.* **2006**, *118*, 4761–4764; *Angew. Chem. Int. Ed.* **2006**, *45*, 4645–4648; e) H. M. Kim, B. R. Cho, *Acc. Chem. Res.* **2009**, *42*, 863–872; f) V. Parthasarathy, S. Fery-Forgues, E. Campioli, G. Recher, F. Terenziani, M. Blanchard-Desce, *Small* **2011**, *7*, 3219–3229; g) S. Yao, K. D. Belfield, *Eur. J. Org. Chem.* **2012**, 3199–3217; h) C. Le Droumaguet, A. Sourdon, E. Genin, O. Mongin, M. Blanchard-Desce, *Chem. Asian J.* **2013**, *8*, 2984–3001.

[3] a) S. Kim, T. Y. Ohulchanskyy, H. E. Pudavar, R. K. Pandey, P. N. Prasad, *J. Am. Chem. Soc.* **2007**, *129*, 2669–2675; b) H. A. Collins, M. Khurana, E. H. Moriyama, A. Mariampillai, E. Dahlstedt, M. Balaz, M. K. Kuimova, M. Drobizhev, V. X. D. Yang, D. Phillips, A. Rebane, B. C. Wilson, H. L. Anderson, *Nat. Photonics* **2008**, *2*, 420–424; c) J. R. Starkey, A. K. Rebane, M. A. Drobizhev, F. Meng, A. Gong, A. Elliott, K. McInnerney, C. W. Spangler, *Clin. Cancer Res.* **2008**, *14*, 6564–6573; d) B. W. Pedersen, T. Breitenbach, R. W. Redmond, P. R. Ogilby, *Free Radical Res.* **2010**, *44*, 1383–1397; e) M. Gary-Bobo, Y. Mir, C. Rouxel, D. Brevet, I. Basile, M. Maynadier, O. Vaillant, O. Mongin, M. Blanchard-Desce, A. Morère, M. Garcia, J.-O. Durand, L. Raehm, *Angew. Chem.* **2011**, *123*, 11627–11631; *Angew. Chem. Int. Ed.* **2011**, *50*, 11425–11429; f) X. Yue, C. O. Yanez, S. Yao, K. D. Belfield, *J. Am. Chem. Soc.* **2013**, *135*, 2112–2115.

[4] L. R. Dalton, P. A. Sullivan, D. H. Bale, *Chem. Rev.* **2010**, *110*, 25–55, and references cited therein.

[5] a) P. J. Campagnola, M.-d. Wei, A. Lewis, L. M. Loewe, *Biophys. J.* **1999**, *77*, 3341–3349; b) L. Moreaux, O. Sandre, S. Charpak, M. Blanchard-Desce, J. Mertz, *Biophys. J.* **2001**, *80*, 1568–1574; c) D. A. Dombeck, M. Blanchard-Desce, W. W. Webb, *J. Neurosci.* **2004**, *24*, 999–1003; d) J. E. Reeve, H. L. Anderson, K. Clays, *Phys. Chem. Chem. Phys.* **2010**, *12*, 13484–13498.

[6] a) J. Zyss, I. Ledoux, *Chem. Rev.* **1994**, *94*, 77–105; b) T. Verbiest, K. Clays, C. Samyn, J. Wolff, D. Reinhoudt, A. Persoons, *J. Am. Chem. Soc.* **1994**, *116*, 9320–9323; c) H. M. Kim, B. R. Cho, *J. Mater. Chem.* **2009**, *19*, 7402–7409, and references cited therein.

[7] G. Argouarch, R. Veillard, T. Roisnel, A. Amar, A. Boucekkine, A. Singh, I. Ledoux, F. Paul, *New J. Chem.* **2011**, *35*, 2409–2411.

[8] Y.-K. Lee, S.-J. Jeon, M. Cho, *J. Am. Chem. Soc.* **1998**, *120*, 10921–10927.

[9] Y. M. Poronik, V. Hugues, M. Blanchard-Desce, D. T. Gryko, *Chem. Eur. J.* **2012**, *18*, 9258–9266.

[10] a) T. Le Bahers, C. Adamo, I. Ciofini, *J. Chem. Theory Comput.* **2011**, *7*, 1144–1152; b) D. Jacquemin, T. Le Bahers, C. Adamo, I. Ciofini, *Phys. Chem. Chem. Phys.* **2012**, *14*, 5383–5388.

[11] A. Willetts, J. E. Rice, D. M. Burland, D. P. Shelton, *J. Chem. Phys.* **1992**, *97*, 7590–7599.

[12] M. de Wergifosse, B. Champagne, *J. Chem. Phys.* **2011**, *134*, 074113.

[13] F. Castet, E. Bogdan, A. Plaquet, L. Ducasse, B. Champagne, V. Rodriguez, *J. Chem. Phys.* **2012**, *136*, 024506.

[14] J. Campo, A. Painelli, F. Terenziani, T. van Regemorter, D. Beljonne, E. Goovaerts, W. Wenseleers, *J. Am. Chem. Soc.* **2010**, *132*, 16467–16478.

[15] V. Rodriguez, D. Talaga, F. Adamietz, J. L. Bruneel, M. Couzi, *Chem. Phys. Lett.* **2006**, *431*, 190–194.

[16] a) O. Quinet, B. Champagne, V. Rodriguez, *J. Chem. Phys.* **2004**, *121*, 4705 – 4710; b) O. Quinet, B. Champagne, V. Rodriguez, *J. Chem. Phys.* **2006**, *124*, 244312.
[17] V. Rodriguez, *J. Raman Spectrosc.* **2012**, *43*, 627 – 636.
[18] V. Rodriguez, M. Couzi, F. Adamietz, M. Dussauze, G. Guery, T. Cardinal, P. Veber, K. Richardson, P. Thomas, *J. Raman Spectrosc.* **2013**, *44*, 739 – 745.
[19] S. Brasselet, J. Zyss, *J. Opt. Soc. Am. B* **1998**, *15*, 257 – 288.
[20] V. Rodriguez, J. Grondin, F. Adamietz, Y. Danten, *J. Phys. Chem. B* **2010**, *114*, 15057 – 15065.
[21] S. P. Karna, M. Dupuis, *J. Comput. Chem.* **1991**, *12*, 487 – 504.
[22] A. Plaquet, M. Guillaume, B. Champagne, F. Castet, L. Ducasse, J.-L. Pozzo, V. Rodriguez, *Phys. Chem. Chem. Phys.* **2008**, *10*, 6223 – 6232.
[23] a) H. Sekino, Y. Maeda, M. Kamiya, K. Hirao, *J. Chem. Phys.* **2007**, *126*, 014107; b) A. Limacher, K. V. Mikkelsen, H. P. Lüthi, *J. Chem. Phys.* **2009**, *130*, 194114; c) R. Kishi, S. Bonness, K. Yoneda, H. Takahashi, E. Botek, B. Champagne, T. Kubo, K. Kamada, K. Ohta, T. Tsuneda, *J. Chem. Phys.* **2010**, *132*, 094107; d) S. I. Lu, C. C. Chiu, Y. F. Wang, *J. Chem. Phys.* **2011**, *135*, 134104.
[24] a) O. Quinet, B. Champagne, B. Kirtman, *J. Mol. Struct. THEOCHEM* **2003**, *633*, 199 – 207; b) A. S. Dutra, M. A. Castro, T. L. Fonseca, E. E. Fileti, S. Canuto, *J. Chem. Phys.* **2010**, *132*, 034307.
[25] Gaussian 09 (Revision A.02), M. J. Frisch, G. W. Trucks, H. B. Schlegel, G. E. Scuseria, M. A. Robb, J. R. Cheeseman, G. Scalmani, V. Barone, B. Mennucci, G. A. Petersson, H. Nakatsuji, M. Caricato, X. Li, H. P. Hratchian, A. F. Izmaylov, J. Bloino, G. Zheng, J. L. Sonnenberg, M. Hada, M. Ehara, K. Toyota, R. Fukuda, J. Hasegawa, M. Ishida, T. Nakajima, Y. Honda, O. Kitao, H. Nakai, T. Vreven, J. A. Montgomery, Jr., J. E. Peralta, F. Ogliaro, M. Bearpark, J. J. Heyd, E. Brothers, K. N. Kudin, V. N. Staroverov, R. Ko-bayashi, J. Normand, K. Raghavachari, A. Rendell, J. C. Burant, S. S. Iyengar, J. Tomasi, M. Cossi, N. Rega, J. M. Millam, M. Klene, J. E. Knox, J. B. Cross, V. Bakken, C. Adamo, J. Jaramillo, R. Gomperts, R. E. Stratmann, O. Yazyev, A. J. Austin, R. Cammi, C. Pomelli, J. W. Ochterski, R. L. Martin, K. Morokuma, V. G. Zakrzewski, G. A. Voth, P. Salvador, J. J. Dannenberg, S. Dapprich, A. D. Daniels, Ö. Farkas, J. B. Foresman, J. V. Ortiz, J. Cioslowski, D. J. Fox, Gaussian, Inc., Wallingford CT, **2009**.

Received: March 3, 2014
Published online on ■■ ■■, 2014

ARTICLES

*F. Castet, M. Blanchard-Desce, F. Adamietz, Y. M. Poronik, D. T. Gryko, V. Rodriguez**

■■ – ■■

Experimental and Theoretical Investigation of the First-Order Hyperpolarizability of Octupolar Merocyanine Dyes

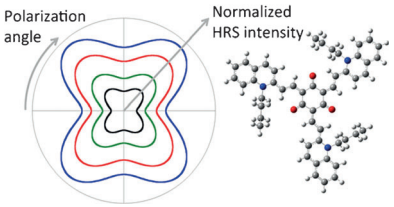

Poles apart: Hyper-Rayleigh scattering (HRS) experiments and quantum chemical calculations are combined to investigate the second-order nonlinear optical responses of a series of three-arm merocyanine derivatives. The figure shows the structure and normalized HRS intensity of one of the four investigated octupolar merocyanines.